Article ID: 1003－6326(2003)05－1247－05

Characterization and photocatalytic activity for methylene blue degradation of iron-deposited TiO_2 photocatalyst①

XU Yue-hua(徐悦华)[1, 2], WANG Liang-yan(王良焱)[1], HUANG Cong(黄 琮)[1], LI Xin-jun(李新军)[1], LI Fang-bai(李芳柏)[3], ZHENG Shao-jian(郑少健)[1], ZHANG Qi(张 琦)[1]
(1. Guangzhou Institute of Energy Conversion, the Chinese Academy of Science, Guangzhou 510070, China;
2. College of Science, South China Agricultural University, Guangzhou 510642, China;
3. Guangdong Institute of Eco-Environment and Soil Science, Guangzhou 510650, China)

Abstract: Iron-deposited TiO_2 was prepared by photo-reducing ferric ions. The photocatalytic activity of methylene blue degradation was enhanced after TiO_2 was deposited with iron, and the optimum $n(Fe)/n(Ti)$ is 0.25%. TiO_2 and iron-deposited TiO_2 are anatase and rutile, and anatase is the dominant crystalline phase. In all samples, the XRD patterns indicate that there are no characteristic peaks of iron to be detected. XPS confirms that Fe^{3+} and Fe^{2+} are present on the surface of 0.5% iron-deposited TiO_2, however they are not susceptible to XRD detection. The thermodynamics analysis shows that the alternative possibility of reduction from the Fe^{3+}/Fe^{2+} couple seems plausible, but Fe^{2+} can not be reduced to Fe. The fluorescence intensity weakens after iron is deposited on TiO_2, because iron deposited traps photo-generated electrons and holes. The fluorescence intensity order of TiO_2 and iron-deposited TiO_2, from strong to weak, is in good agreement with that of photocatalytic reactiveness TiO_2 and iron-deposited TiO_2, from low to high.

Key words: methylene blue; iron deposited TiO_2; TiO_2; photocatalytic degradation
CLC number: O 643.32; TQ 453.2 **Document code:** A

1 INTRODUCTION

Semiconductor photocatalysis has received a lot of attention as a promising technique for the total destruction of organic compounds in the polluted air and wastewater. The basic principle of semiconductor photocatalysis involves photon-generated electrons and holes migrating to the surface and serving as redox sources that react with adsorbed reactants leading to the destruction of pollutants. Titanium dioxide appears to be the most practical photocatalyst among the semiconductors for widespread environmental application. The photocatalytic activity depends on the surface charge carrier transfer rate and the electron-hole recombination rate. Indeed TiO_2, due to its bandgap energy (for anatase ≈ 3.2 eV, for rutile ≈ 3.0 eV), catalyzes the oxidation of organic pollutants in the presence of near UV radiation more than or equal to 387 nm. In general, larger band-gap energy should result from larger thermodynamic driving forces and faster charge-carrier transfer rates. However, high recombination rates of the electron-hole pairs photo-produced in the TiO_2 interface tend to limit the relative photo-efficiencies. In order to enhance the photocatalytic activity of TiO_2, extensive research is underway to modify TiO_2, such as the binary metal oxide[1], transition metal-ions-doped[2], precious metal-deposited[3], surface sensitization[4], etc.

Different methods were employed to prepare iron-deposited titanium specimens and binary mixed oxides. The photocataclytic activity of TiO_2 doped with ferric ions, prepared by wet impregnation and coprecipitation, has been shown to be feasible in the visible light for the dinitrogen photoreduction to ammonia[5]. Doping of TiO_2 with Fe (III) was reported to improve photocatalytic properties and enhance visible light response[2]. Fe_2O_3/TiO_2 was prepared by impregnation method, and the photocatalytic oxidation activity of phenol was improved[6]. Pal et al[7, 8] prepared TiO_2/Fe_2O_3 binary mixed oxides by sol-gel impregnation using metal alkoxide precursors, and found that the sample sintered at 500 ℃ shows highest activity for the degradation of aqueous solution of O-Cresol. Coupled Fe_2O_3/TiO_2 nanometer powders were prepared by adding TiO_2 in $Fe(OH)_3$ colloid, and the photocatalytic activity for methamidophos degradation was enhanced when $n(Fe)/n(Ti)$ was

① **Foundation item:** Project (010873 a) supported by Guangdong Natural Science Foundation of China and project (A3040301) supported by Guangdong Science & Technology Development Foundation of China
Received date: 2002－12－26; **Accepted date:** 2003－05－30
Correspondence: XU Yue-hua, Associate professor; Tel: +86-20-85281989; E-mail: xuyuehua@scau.edu.cn

less than 0.3%[9]. The present study evaluates the activity of TiO_2 and iron deposited TiO_2 for the photocatalytic degradation of methylene blue as a model pollutant. We tried to explore the chemical composition and electronic structure of TiO_2 and iron deposited TiO_2, and make a detailed investigation on elucidating the mechanism of the iron action on the photoreactivity of TiO_2.

2 EXPERIMENTAL

Chemicals and solvents were at least reagent grade and were used as received.

2.1 Preparation

40 mL of tetrabutyl titanate was dissolved in 200 mL absolute alcohol. The transparent solution A was formed during the first few minutes. Meanwhile the solution B was prepared by adding 40 mL of glacial acetic acid to 40 mL distilled water and 160 mL anhydrous alcohol with vigorous stirring. Then a transparent colloidal solution was obtained by adding dropwise solution A to the aqueous solution B with vigorous stirring. After the solution was changed into gel, dried it in a vacuum drying oven at 65 ℃. Dry gel was milled in an agate mortar, and subsequently calcined in air at 700 ℃ for 1 h to acquire the TiO_2 sample.

TiO_2 deposited with iron was prepared by photoreducing ferric ions. The $n(Fe)/n(Ti)$ of the samples were 0.15%, 0.25%, 0.5%, 1.0% and 2.0% respectively. The preparation of each sample was carried out as follows: 400 mL distilled water, 2 g TiO_2, the required amount of glacial acetic acid and aqueous solutions of $Fe(NO_3)_3$ were mixed and then reduced by a 125 W high-pressure mercury lamp for 40 min with a 150 cm^3/min stream of N_2. Then it was filtered with a microfilteration membrane and dried at 338 K to get the final sample.

2.2 Photocatalytic activity tests

Aqueous slurry was prepared by adding 360 mg TiO_2 or Iron-deposited TiO_2 to 400 mL solution containing methylene blue at 10^{-3}% respectively. Then irradiation was performed with a 125 W high-pressure mercury lamp to the aqueous slurries after it was stirred and bubbled with humid oxygen for 20 min and the lamp was warmed up for 20 min. At given irradiation time intervals, the dispersion was extracted and centrifuged to separate the TiO_2 particles. The filtrate was analyzed by UV-vis spectra with a spectrophotometer and measuring its absorbance at 664nm. All experiments were performed at room temperature and at natural pH 6.

2.3 Characterization

The X-ray diffraction(XRD) patterns were obtained at room temperature with a S/MAX IIIA diffractometer using Ni-filtered Cu K_α radiation (λ= 0.154 18 nm). The step scans were taken over the range 2θ from 15° to 65°. The mean crystallite diameters were estimated by application of the Scherrer equation.

The XPS spectra were collected by a PHI Quantum 2000 Scanning ESCA Microprobe with a pass energy of 20 eV, and the excitation of the spectra was performed by means of monochromatized Al K_α radiation. Correction of the energy shifts due to static charging of the samples was accomplished by referencing to the C 1 s line from the residual pump-line oil contamination taken at 285.0 eV.

3 RESULTS AND DISCUSSION

3.1 Photocatalytic results

The experimental results of the methylene blue photocatalytic degradation are shown in Fig. 1. Under the reported experimental conditions, the photocatalytic degradation reaction kinetics of methylene blue follows first apparent order, that is $\lg c_0/c = kt$, in which c_0 is the initial concentration of methylene blue, c is the concentration of methylene blue at any time, k is the reaction rate constant.

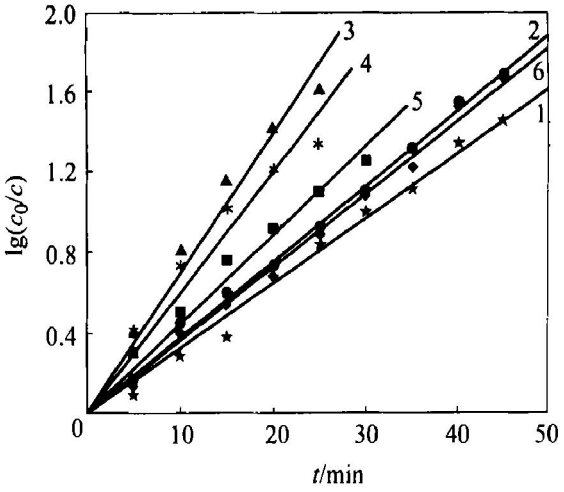

Fig. 1 Relation between $\lg(c_0/c)$ and t of amples for methylene blue photocatalytic degradation
1—TiO_2; 2—0.15% iron-deposited TiO_2;
3—0.25% iron-deposited TiO_2;
4—0.5% iron-deposited TiO_2;
5—1% iron-deposited TiO_2; 6—2% iron-deposited TiO_2

The photocatalytic activity of all iron-deposited TiO_2 for methylene blue degradation is higher than that of TiO_2. The activity, however, does not parallel with the iron content. The photocatalytic activity increases with the amount of iron on TiO_2 increasing, and then diminishes with the amount of iron decreasing. The highest photocatalytic activity was obtained

in an iron molar concentration of 0.25%.

3.2 X-ray diffraction analysis

Table 1 shows the phase and crystal size of TiO_2 and iron-deposited TiO_2. XRD results show that TiO_2 and iron-deposited TiO_2 are anatase and rutile, and anatase was the dominant phase. Anatase(100)/rutile(8) is the ratio of the main peak intensity of anatase and that of rutile. The proportion of anatase phase in TiO_2 is larger than that in iron-deposited TiO_2, perhaps anatase is changed into rutile during the photo-reduction.

Table 1 Phase and crystallite size of TiO_2 and iron-deposited TiO_2

Photocatalyst	Phase	Crystal size/nm
TiO_2	anatase(100)/rutile(8)	30
0.25% iron deposited TiO_2	anatase(100)/rutile(19)	32
0.5% iron deposited TiO_2	anatase(100)/rutile(18)	32
2% iron deposited TiO_2	anatase(100)/rutile(15)	34

The polycrystalline X-ray diffraction patterns of TiO_2 and 2% iron-deposited TiO_2 are shown in Fig. 2. In all samples, the XRD patterns indicate that no characteristic peaks of iron were detected even at the highest iron-deposited on TiO_2, i.e. 2% iron-deposited TiO_2.

The absence of iron X-ray diffraction peaks may be attributed to the fact that the iron species are present as a highly dispersed or amorphous state on the surface of TiO_2. However, the existence possibility of iron size less than 4 nm cannot be ruled out in the photocatalysts, which is beyond the detection capacity of the powder X-ray diffraction technique. On the surface of TiO_2, the iron may be present as single particle or aggregate that is not susceptible to XRD detection.

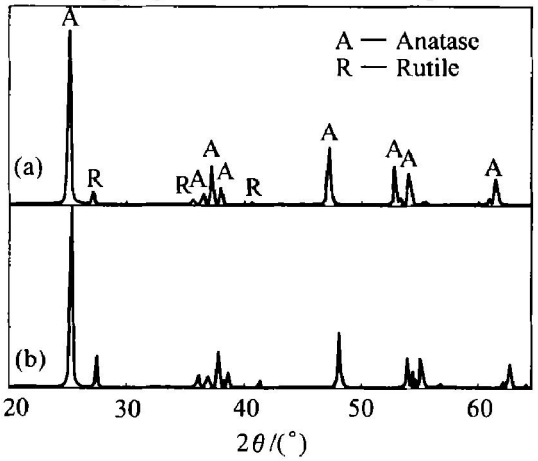

Fig. 2 X-ray diffraction patterns of TiO_2 and 2% iron-deposited TiO_2
(a) —TiO_2; (b) —2% iron-deposited TiO_2

3.3 XPS study

Fig. 3 shows the XPS survey spectra of 0.5% iron-deposited TiO_2. O, C, Ti, and Fe elements are present on the surface of 0.5% iron-deposited TiO_2, and C element is attributed to the residual pump-line oil contamination. The analysis result indicates that there is 1.5% iron on the surface of 0.5% iron-deposited TiO_2. There are two reasons for this result:

1) Because the amount of iron on TiO_2 is small, the Signal/Noise ratio is not big. It is not easily to determine exactly the amount and states of iron on the surface of TiO_2.

2) Most of iron is present on the surface of TiO_2.

The Fe $2p_{3/2}$ core level spectra of 0.5% iron-deposited TiO_2 is shown in Fig. 4. The Fe $2p_{3/2}$ 710.4 eV peak is assigned to Fe^{3+}, while the Fe $2p_{3/2}$ 709.6 eV peak can be attributed to Fe^{2+}. Because the signal intensity is low, it is difficult to calculate exactly the amount on different states of iron on the surface of TiO_2.

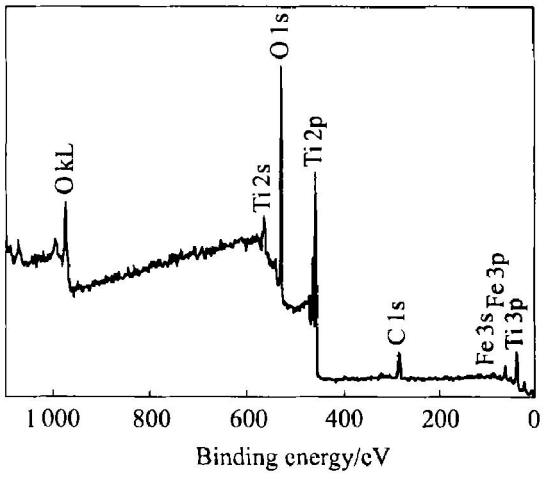

Fig. 3 XPS survey spectra of 0.5% iron-deposited TiO_2

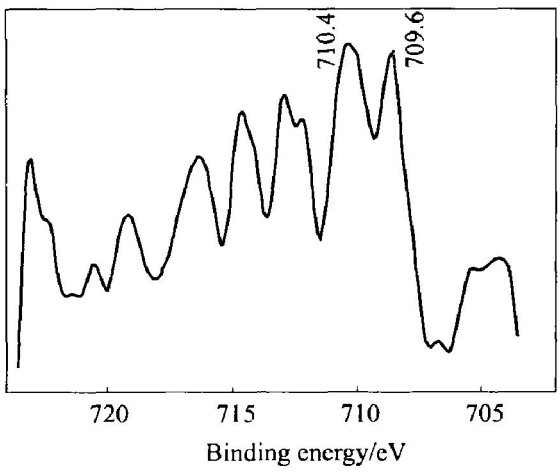

Fig. 4 Fe $2p_{3/2}$ core level spectra of 0.5% iron-deposited TiO_2

When TiO_2 is exposed to light of energy equal to or greater than the bandgap energy, an electron is excited from the TiO_2 valence band into the TiO_2 conduction band, leaving a hole behind. The photo-induced electrons are good reductants. If a suitable scavenger (acetic acid) is available to trap the hole, and subsequent reduction reaction may occur. Only if the relevant potential level of the acceptor species, ferric ion (Fe^{3+}), is required to be below (more positive than) the conduction band potential of the semiconductor on thermodynamics, Fe^{3+} can be reduced to Fe^{2+}. The resultant of reduction states of iron on TiO_2 may be explained by the following reactions:

$$Fe^{3+} + 3e \rightarrow Fe \qquad \varphi^0 = -0.037\ V \qquad (1)$$

$$Fe^{2+} + 2e \rightarrow Fe \qquad \varphi^0 = -0.447\ V \qquad (2)$$

$$Fe^{3+} + e \rightarrow Fe^{2+} \qquad \varphi^0 = 0.771\ V \qquad (3)$$

The oxidation potential of Fe^{3+} (Eqn. (1)) approximately equals to the reduction potential of the photoinduction electron[10], so Fe^{3+} is hardly reduced to Fe. However, Fig. 4 shows that Fe is not present on the surface of 0.5% iron-deposited TiO_2, because the Fe $2p_{3/2}$ peak at lower binding energy is situated at about 707 eV[11]. The alternative possibility of reduction from the Fe^{2+}/Fe couple does not seem plausible (Eqn. (2)), but Fe^{3+} can easily be photo-reduced to Fe^{2+} (Eqn. (3)). Therefore, the irradiation of the light of 365 nm wavelength onto the suspensions of TiO_2 in aqueous solution of ferric salts and acetic acid led to the evolution of the deposition of Fe^{3+} and Fe^{2+} onto the surface of TiO_2 (Fig. 4), and the oxidation of acetic acid.

3.4 Fluorescence spectra

Fig. 5 shows the fluorescence spectra (λ_{exc} = 267.0 nm). A fluorescence band of 350 – 525 nm occurs. Increasing amounts of iron do not change its spectral position. The intensity, however, changes with increasing the amount of iron deposited on TiO_2. Following the arguments given in reference [12] that the observed fluorescence could be ascribed to the recombination of photoproduced charge carriers on the surface of TiO_2.

The coexistence of Fe^{3+} and Fe^{2+} at iron-deposited TiO_2 influences the photocatalytic activity by altering the electron-hole pair recombination rate through the following process:

electron trap $\quad Fe^{3+} + e^- \rightarrow Fe^{2+}$

hole trap $\quad Fe^{2+} + h^+ \rightarrow Fe^{3+}$

Trapping either an electron or a hole alone is ineffective because the immobilized charge species quickly recombine with its mobile counterpart[2]. The trapped hole embodied in Fe^{3+} has longer lifetime due to the immobilized electron in Fe^{2+}. Then the trapped charge carriers lead to a series of photocatalytic reactions, so the photocatalytic activity of

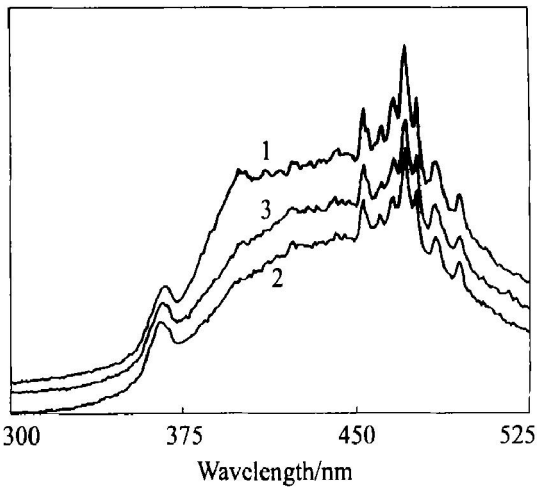

Fig. 5 Fluorescence spectra of pure TiO_2 and different $n(Fe)/n(Ti)$ iron-deposited TiO_2
1—TiO_2; 2—0.25% iron-deposited TiO_2; 3—0.5% iron-deposited TiO_2

iron-deposited TiO_2 are related to the iron deposited trap amount. Fig. 5 shows that the fluorescence intensity of iron-deposited TiO_2 is weaker than that of TiO_2. The weak fluorescence intensity of iron-deposited TiO_2 indicates that the recombination efficiency of charge carriers is lower than that of TiO_2. This means that the photo-excited electron-hole pair on the surface of iron-deposited TiO_2 is separated effectively. The fluorescence intensity order of TiO_2 and iron-deposited TiO_2, from strong to weak, is in good agreement with that of photocatalytic reactive TiO_2 and iron-deposited TiO_2, from low to high.

4 CONCLUSIONS

The photocatalytic activity for methylene blue degradation was enhanced after TiO_2 was deposited with iron by photo-reducing ferric ions, and the optimum iron molar concentration on TiO_2 is 0.25%. TiO_2 and iron-deposited TiO_2 are anatase and rutile, and anatase was the dominant crystalline phase. In all iron-deposited TiO_2, the iron is present as single particle or aggregate, which is beyond the detection capacity of the powder X-ray diffraction technique, on the surface of TiO_2. Fe^{3+} and Fe^{2+} coexist on the surface of 0.5% iron-deposited TiO_2, and the thermodynamics analysis shows that the alternative possibility of reduction from the Fe^{3+}/Fe^{2+} couple seems plausible, but Fe^{2+} can not be photo-reduced to Fe. The fluorescence intensity weakens after iron deposited on TiO_2 because Fe^{3+} and Fe^{2+} at iron-deposited TiO_2 act as electron and hole traps, respectively. The fluorescence intensity order of TiO_2 and iron-deposited TiO_2 is in good agreement with that of photocatalytic reactivity TiO_2 and iron-deposited TiO_2.

REFERENCES

[1] Vogel R, Hoyer P, Weller H. Quantum-sized PbS, CdS, Ag_2S, Sb_2S_3, and Bi_2S_3 particles as sensitizers for various nanoporous wide-bandgap semiconductors[J]. J Phys Chem, 1994, 98(12): 3183 - 3189.

[2] Choi W, Termin A, Hoffmann M R. The role of metal ion dopants in quantum-sized TiO_2: correlation between photoreactivity and charge carrier recombination dynamics[J]. J Phys Chem, 1994, 98(51): 13669 - 13679.

[3] Gao Y M, Lee W, Trehan R, et al. Improvement of photocatalytic activity of titanium (IV) oxide by dispersion of Au on TiO_2[J]. Mat Res Bull, 1991, 26(12): 1247 - 1254.

[4] WU Tai-xing, LIU Guang-ming, ZHAO Jin-cai, et al. Photoassisted degradation of dye pollutants. V. Self-photosensitized oxidative transformation of rhodamine B under visible light irradiation in aqueous TiO_2 dispersions [J]. J Phys Chem, 1998, 102(30): 5845 - 5851.

[5] Soria J, Conesa J C, Augugliaro V, et al. Dinitrogen photoreduction to ammonia over titanium dioxide powders doped with ferric ions[J]. J Phys Chem, 1991, 95 (1): 274 - 282.

[6] JIAN Pan-ming, XIA Ya-mu, LI De-hong, et al. Study on synthesis, characterization and catalytic performance of doped TiO_2 nanosized powder[J]. Chinese J Catal, 2001, 22 (2): 161 - 163. (in Chinese)

[7] Pal B, Hata K, Goto K. Photocatalytic degradation of o-cresol sensitized by iron-titan binary photocatalysts[J]. J Mole Catal A: Chemical, 2001, 169(1): 147 - 155.

[8] Pal B, Sharon M, Nogami G. Preparation and characterization of TiO_2/Fe_2O_3 binary mixed oxides and its photocatalytic properties[J]. Mater Chem and Phys, 1999, 59(2): 254 - 261.

[9] XU Yue-hua, GU Guo-bang, LI Xin-jun. Preparation, characterization and photocatalytic reactivity of coupled Fe_2O_3/TiO_2 nanometer powder[J]. J South China University of Technology, 2001, 29(11): 76 - 80. (in Chinese)

[10] ZHANG Peng-yi, YU Gang, JIANG Zhan-peng. Review of semiconductor photocatalyst and its modification [J]. Advances in Environ Sci, 1997, 5(3): 1 - 10. (in Chinese)

[11] LIU Wei-qiao, SUN Gui-da. Research Methods of Solid Catalyst [M]. Beijing: Petrochemical Industry Press, 2000. 210. (in Chinese)

[12] Hasselbarth A, Eychmuller A, Eichberger R, et al. Chemistry and photophysics of mixed CdS/HgS colloids [J]. J Phys Chem, 1993, 97(20): 5333 - 5340.

(Edited by LI Yan-hong)